Electro-thermally tunable reflective colors in a self-organized cholesteric helical superstructure

Po-Chang Wu[1], Guan-Wei Wu[2], Ivan V. Timofeev[3, 4], Victor Ya. Zyryanov[3], and Wei Lee[1,*]

[1]*Institute of Imaging and Biomedical Photonics, College of Photonics, National Chiao Tung University, Guiren Dist., Tainan 71150, Taiwan*

[2]*Institute of Lighting and Energy Photonics, College of Photonics, National Chiao Tung University, Guiren Dist., Tainan 71150, Taiwan*

[3]*Kirensky Institute of Physics, Federal Research Center "Krasnoyarsk Scientific Center", Siberian Branch of the Russian Academy of Sciences, Krasnoyarsk 660036, Russia*

[4]*Laboratory for Nonlinear Optics and Spectroscopy, Siberian Federal University, Krasnoyarsk 660041, Russia*

**Corresponding author: wlee@nctu.edu.tw*

Received Month X, XXXX; revised Month X, XXXX; accepted Month X, XXXX; posted Month X, XXXX (Doc. ID XXXXX); published Month X, XXXX

We propose to dynamically control the reflective color of a cholesteric liquid crystal (CLC) by electrically tuning the center wavelength (λ_c) of the bandgap. The CLC, sandwiched in a planar-aligned cell with indium–tin-oxide electrodes, possesses negative dielectric anisotropy and thermo-responsive spectral properties. The helix in the Grandjean planar state subject to a vertically applied voltage should be undisturbed in that the long molecular axis is initially perpendicular to the direction of the electric field. Surprisingly, when the frequency of the applied voltage is higher than a critical value, λ_c of the CLC cell varies as a function of the voltage. The underlying mechanism is the voltage-induced temperature change through dielectric heating in the frequency regime of pseudo-dielectric relaxation, attributable to the significant equivalent resistance–capacitance circuit of the cell due to the use of electrode layers with finite conductance. The driving voltage enabling the tuning of λ_c in the entire visible spectrum is as low as 12 V_{rms} in a 5-μm-thick cell at a frequency of 2 MHz. The proposed CLC cell exhibiting a broad electrically tunable spectral range from near infrared to ultraviolet holds great promise for developing tunable photonic devices such as multicolor reflectors, filters, and sensors.

OCIS codes: (160.3710) Liquid crystals; (160.1585) Chiral media; (230.2090) Electro-optical devices; (230.3720) Liquid-crystal devices

1. INTRODUCTION

Cholesteric liquid crystals (CLCs) organized in self-assembled, periodically helical superstructures are known as a class of one-dimensional chiral photonic crystal. In the Grandjean planar (P) state a CLC is characterized by the so-called Bragg bandgap in a specific wavelength region, enabling the reflection of selective circularly polarized light with the same handedness as that of the CLC helix. This unique feature permits CLCs to be promising for the development of a variety of photonic devices such as reflective displays, reflectors, lasers, and sensors [1–4]. More attractively, dynamic control of CLC bandgap properties is attainable, permitting CLC photonic devices with variable optical properties. The center wavelength (λ_c) of the CLC bandgap is determined by the helical pitch (p) as well as the ordinary (n_o) and extraordinary (n_e) refractive indices of the nematic host, according to the relation $\lambda_c = p \cdot (n_e + n_o)/2$ [5]. As such, a good number of studies of tunability of λ_c or tunable reflective color in CLCs have been proposed via the control of helical pitch by external stimuli. For instance, CLCs with thermo-responsive bandgap properties have been obtained on the basis of the temperature dependency of LC phase transition [6], the helical twisting power (HTP) of the chiral dopant [7], and the mixture solubility [8]. Employment of photo-responsive chiral switches as dopants in CLCs has also been suggested for realizing variable and rewritable λ_c by light irradiations thanks to the tunable HTP via the process of photo-induced *trans–cis* isomerizations [9]. On the other hand, electrical tuning of λ_c would be preferable for practical applications, because of the ease of operation and high compatibility of the CLC cell with modern optoelectronic devices. Considering a CLC cell subject to a vertical electric field, most of recent electrical-tuning approaches have been developed using negative nematic LCs — namely, nematic LCs with negative dielectric anisotropy ($\Delta\varepsilon < 0$)—as the host material to prevent helical distortion by the applied voltage. With a direct-current (DC) voltage applied to a CLC consisting of chiral additives in negative LC, wavelength tuning has been asserted and examined in terms of the voltage-induced electrohydrodynamic instability [10], mechanical cell-gap bending [11], and defect annealing [12]. Alternatively, Choi et al. proposed to further exploit ferroelectric LC as electrically commanded aligning surfaces [13] or as dopants [14] in a negative CLC cell to achieve bandgap tuning by alternating-current (AC) voltages. However, the tunable wavelength ranges of the bandgap are quite limited and the voltages required are generally too high (> 100 V by either DC or AC voltage) by the above-mentioned electrical-tuning approaches, thus hindering their practical uses. In a special case, Xiang et al. demonstrated electrically tunable selective reflection from ultraviolet (UV) to visible and infrared (IR) in an oblique helicoid state rather than the typical P state by doping proper amounts of the bent-shape molecules CB7CB and CB6OCB into a CLC [15].

Different from all aforementioned studies, in this work we propose a state-of-the-art approach based on the electro-thermal effect, allowing the tunability of the reflective color in a wide wavelength range, covering the entire visible spectrum, by AC voltage applied across a negative CLC that is confined in a planar-aligned cell with indium–tin-oxide (ITO) electrodes. Here the CLC is designed to intrinsically possess thermo-responsive bandgap properties. When the frequency of applied voltage goes beyond a critical value, our results indicated that λ_c of the reflection band can be electrically tuned by varying either the amplitude or the frequency of the AC voltage. The results are complemented by both dielectric spectroscopy and IR thermography, affirming the increase in cell temperature through the induction of dielectric heating by the applied voltage. In general, dielectric heating in a dielectric medium stems from absorption of electromagnetic energy through rotation of molecular dipoles and its efficacy becomes remarkable in the frequency regime of dielectric relaxation. Because the dielectric relaxation from molecular dipole reorientation of a typical LC does not occur in the kHz-to-MHz frequency regime, the dielectric heating effect in sandwich-type LC cells to date has only been discussed in dual-frequency LC whose relaxation frequency (viz., the crossover frequency) is about tens of kHz [16–18]. In our case, where a common negative CLC is employed, the dielectric heating is primarily governed by the pseudo-relaxation from the ITO effect due to the generation of losses from the cell comprising electrodes with non-zero resistance. As a result, the λ_c of the proposed negative CLC with superior electro-thermal properties can vary from 780 nm at 0 V_{rms} to 380 nm at merely 12 V_{rms} at 2 MHz, manifesting a wider tunable wavelength range entailing much lower driving voltage in comparison with those by most of current electrical tuning methods.

2. EXPERIMENT

The CLC used was prepared by incorporating 45 wt% of the left-handed chiral additive S-811 (Merck) into the negative nematic host MLC-6608 (Merck) to induce the SmA–CLC phase transition so as to display thermal-responsive spectral properties in the CLC phase. MLC-6608 has birefringence $\Delta n = 0.083$ (measured at the wavelength of 589 nm and temperature of 20 °C) and dielectric anisotropy $\Delta\varepsilon = -4.2$ (at the frequency f of 1 kHz and temperature of 20 °C). The phase sequence of the mixture is SmA–21 °C–CLC–39 °C–Isotropic, as determined by optical textures using a polarizing optical microscope (Olympus BX51) at various temperatures in a heating process. The CLC was heated to the isotropic phase and stirred for 2 h to ensure homogeneous blending, followed by its injection into an empty cell by capillary action. The empty cell is composed of two glass substrates; each substrate bearing an ITO electrode was spin-coated with an aligning layer (SE-2170) to promote planar alignment of LC molecules and, thus, the initial P state in the CLC phase. The cell gap and the effective electrode area of the cell are $d = 5 \pm 0.5$ μm and $A = 1$ cm^2, respectively. In general, a LC cell is made by sandwiching a LC between two ITO-covered substrates. When the resistivity of the ITO is not negligible the equivalent circuit of such a sandwich-type cell geometry can be represented by a resistance arising from the electrode layers and a capacitance contributed by the LC layer in series. As such, it has been found that the cell applied with voltages at specific frequencies will generate a certain amount of dielectric losses, leading to the induction of a pseudo-dielectric relaxation in the complex dielectric spectra [19]. The corresponding relaxation frequency (f_{PR}) can be defined as:

$$f_{PR} = 1/(2\pi R_{ITO} C_{cell}) \quad (1)$$

where R_{ITO} ~310 Ω is the resistance of the ITO and $C_{cell} = \varepsilon_0\varepsilon_s(A/d)$ is the capacitance of the cell. Because the vacuum permittivity $\varepsilon_0 = 8.854 \times 10^{-12}$ F·m^{-1}, $A = 1$ cm^2 and $d = 5$ μm are all constants, the values of C_{cell} as well as f_{PR} are primarily dominated by the dielectric constant of the material (ε_s) filled in the cell. In the case of an empty cell with an air gap ($\varepsilon_s = 1$), C_{cell} measured is ~0.18 nF and f_{PR} as calculated by Eq. (1) is ~2.85 MHz. Note that this unique pseudo-dielectric relaxation is the key responsible for the dielectric heating by an external voltage in this study.

All measurements were carried out at a given surrounding temperature (T_s = 22 °C or 23 °C as designated) without using a hot stage unless specified. Spectral properties of the cell in the wavelength regime between 380 nm and 800 nm were monitored by transmission spectroscopy using a fiber-optic spectrometer (Ocean Optics HR2000+) in conjunction with a halogen light source (Ocean Optics HL2000). No polarizer was employed in the spectral measurement. To investigate the dielectric heating effect and electro-thermal properties of the CLC cell, dielectric spectra and the change in cell temperature (ΔT) as a function of the applied voltage (V) were respectively acquired with a high-precision LCR meter (Agilent E4980A) and a non-contact IR thermometer (precisely, IR camera FLIR ThermaCam® P25). External voltages in the sinusoidal waveform with controllable amplitudes (from 0.05 V_{rms} to 15 V_{rms}) and frequencies (from 20 Hz to 2 MHz) were specifically supplied by the same LCR meter to prevent from errors under various voltage conditions caused by different instruments.

3. RESULTS AND DISCUSSION

Figure 1 illustrates the temperature-dependent bandgap properties and optical textures at four given temperatures of the CLC cell without voltage applied. Here, the cell was placed on a hot stage (Linkam-LTS120E) to precisely control the cell temperature. The experimental data, as shown in Fig. 1(a), indicate that the reflection band blue-shifted gradually with rising temperature (T), varying from λ_c = 760 nm at T = 23 °C to λ_c = 380 nm at T = 32 °C. This led to the change in color of the reflective optical texture at various temperatures, appearing red (λ_c = 760 nm) at 23 °C, orange (λ_c = 610 nm) at 23.8 °C, green (λ_c = 512 nm) at 25 °C, and navy (λ_c = 397 nm) at 29.4 °C (see Fig. 1(b)). When using the chiral material S-811 as the dopant to form a CLC with a SmA–CLC phase transition, similar results to Fig. 1(a) have also been obtained in CLCs with distinct nematic hosts [12, 20] and this phenomenon has been interpreted by the temperature dependence of the twist elastic constant [6]. Such temperature-dependent spectral behavior can be fitted by Keating's theory, expressed as [21]:

$$\lambda_c(T) = \gamma \frac{T_0}{T}\left(1 + \frac{\beta}{T - T_0}\right)^2, \quad (2)$$

where γ and β are fitting parameters, T is in Kelvin (K), and $T_0 < T$ is the SmA–CLC phase transition temperature. We simulated temperature-dependent λ_c of our cell in the CLC phase temperature range between 22 °C and 39 °C by fitting

the experimental data (open circles) given in Fig. 1(a) and, with the best-fit parameters of $\gamma = 321.58$ nm and $\beta = 1.08$ K, the simulated curve (solid line) suggests that the proposed CLC cell can possess a widely tunable range of λ_c by suitable temperature control, from 1392 nm (IR) at 22 °C to 340 nm (UV) at 39 °C.

To discuss the correlation between the "pseudo-dielectric relaxation" and the voltage-induced dielectric heating, Fig. 2(a) firstly displays the complex dielectric spectra of the pure LC (MLC-6608) and the CLC (MLC-6608 + 45-wt% S-811) cells representatively at T = 23 °C. Because the orientation of the LC molecules having $\Delta\varepsilon < 0$ remains unchanged in a vertical electric field, the profile of the dielectric spectrum is independent of the amplitude of the probe voltage. When the resistivity of the ITO material is

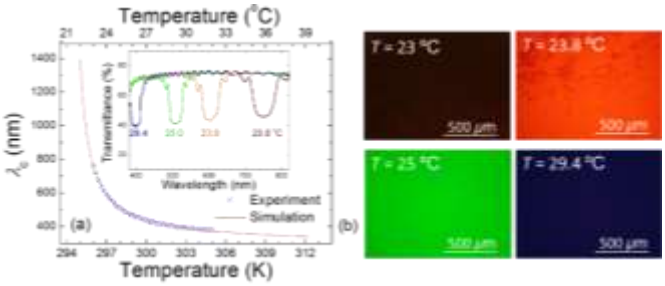

FIG. 1. Temperature-dependent (a) λ_c of the experimental (open circles) and simulated (solid line) results and (b) optical textures of the cell in the CLC phase observed in the reflection mode at four distinct temperatures. Inset in (a) is the transmission spectra at various temperatures.

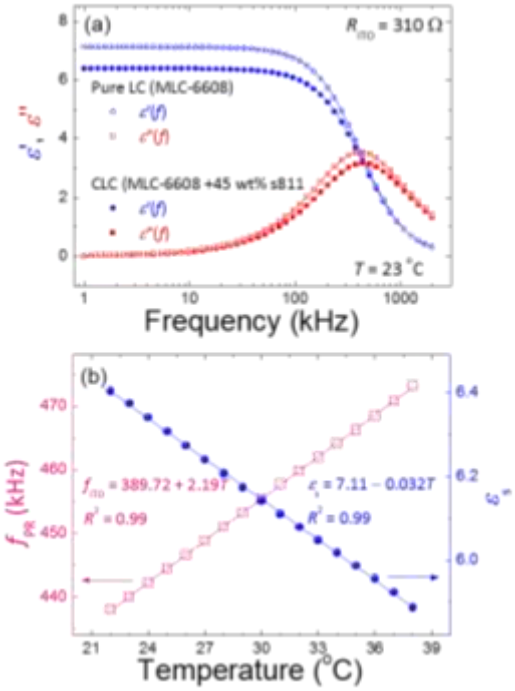

FIG. 2. (a) Experimental and simulated complex dielectric spectra of the pure LC (MLC-6608) and the CLC (MLC-6608 + 45-wt% S-811) cells at T = 23 °C and (b) temperature dependence of deduced static dielectric constant ε_s and relaxation frequency f_{PR} of the pseudo-dielectric relaxation of the LC cell in the CLC phase.

nontrivial, which is truly the case, a resistance–capacitance circuit is produced in a sandwich-type cell, resulting in energy losses and, in turn, a pseudo-dielectric relaxation [19]. Now that the polarization contributed by space charge is excluded at high frequencies (> kHz) and the orientational polarization relaxation of a negative LC typically occurs beyond MHz [18], the single Debye-type relaxation detected in the complex dielectric spectra of either cell is undoubtedly attributable to the use of the ITO cell. Referring to the Debye model, the real- (ε') and imaginary-part (ε'') dielectric functions of this relaxation can be described by:

$$\varepsilon' = \varepsilon_\infty + \frac{(\varepsilon_s - \varepsilon_\infty)}{1+\omega^2\tau_{PR}^2} \tag{3}$$

and

$$\varepsilon'' = \frac{(\varepsilon_s - \varepsilon_\infty)\omega\tau_{PR}}{1+\omega^2\tau_{PR}^2}, \tag{4}$$

respectively, where $\omega = 2\pi f$ is the angular frequency, τ_{PR} is the relaxation time of this pseudo-dielectric behavior inversely related to the relaxation frequency f_{PR} in accordance with $2\pi f_{PR}\tau_{PR} = 1$, and ε_s and ε_∞ are dielectric permittivities at the low- and high-frequency limits, respectively. By fitting the experimental data of Fig. 2(a) to either Eq. (3) or Eq. (4), ε_s and f_{PR} of the CLC cell at T = 23 °C are deduced to be ~6.4 and ~440 kHz, respectively. In accordance with Eq. (1), ε_s of the cell is changed from 1 to 6.4 after the injection of CLC so that f_{PR} can be calculated by f_{PR} = 2.85/6.4 ~ 445 kHz, which is in good agreement with that of the fitted result (i.e., f_{PR} = 440 kHz). It can also be found that the profile of pseudo-dielectric relaxation of the CLC cell is nearly identical to that of the pure LC counterpart, indicating that adding S-811 into MLC-6608 is insufficient to modify the relaxation frequency (from f_{PR} = 417 kHz in the pure LC to f_{PR} =440 kHz in the CLC) due to the limited variation in ε_s. This also implies that the dielectric relaxation from LC molecules cannot be shifted to the investigated frequency regime even when doping 45 wt% of S-811 into the LC. Figure 2(b) unambiguously reveals the temperature dependence of f_{PR} of the CLC cell. One can see that f_{PR} varies linearly with T and it shows a 35-kHz variation only, from f_{PR} = 438 kHz (at T = 22 °C) to f_{PR} = 473 kHz (at T = 38 °C). This temperature-dependent relaxation behavior is in agreement, to the first order of the binomial expansion, with the decrease in ε' with increasing T (from 6.4 at T = 22 °C to 5.9 at T = 38 °C). It should be noted here that the change in f_{PR} as a function of the temperature also follows the Arrhenius equation with the activation energy of 0.038 eV.

Figure 3(a) depicts the f dependence of the steady-state cell temperature at V = 15 V_{rms} measured by an IR camera. Here, each IR image was taken after the application of a given voltage to the cell for 8 min to ensure that the cell temperature became saturated or time-independent. For this measurement, T_s was controlled at 23 °C and the temperature increase ΔT is defined as $T - T_s > 0$. The control of cell temperature by applied voltage was directly confirmed by IR thermography, revealing image color changes from blue in the field-off state or at f = 1 kHz (T = 23 °C) to green at f = 600 kHz (T = 32 °C) and to yellow at f = 2 MHz (T = 37.7 °C), as shown in the insets of Fig. 3(a).

Figure 3(a) indicates that there exists a critical frequency (f_0) that triggers the onset of temperature increase with increasing frequency. In the case of V = 15 V_{rms}, ΔT starts to increase with rising frequency beyond 24.5 kHz, reaching ΔT ~14.7 °C (i.e., T = 37.7 °C) at f = 2 MHz. In considering the relation between the heat generation and the dielectric properties of a LC cell, we attempt to elucidate the result of Fig. 3(a) in terms of the temperature elevation from the dielectric heating effect by the following time-varying equation [16]:

$$\Delta T = \left(\frac{V^2 A\varepsilon_0(\varepsilon_s - \varepsilon_\infty)}{d(C+ht)}\right)\left(\frac{\tau_R \omega^2 t}{1+\omega^2\tau_R^2}\right), \quad (5)$$

where t is the dielectric heating time, ε_0 is the dielectric constant in vacuum and C and h are the average heat capacity and the specific heat conductivity of the cell, respectively. In contrast to τ_{PR} (f_{PR}), τ_R (f_R) is the relaxation time (frequency) of the principal dielectric relaxation that dominates the voltage-induced dielectric heating. To date, Eq. (5) has only been exploited for explaining the dielectric heating behaviors of a LC cell from the dielectric relaxation of LC molecules [16, 17]. Nevertheless, because the origin of Eq. (5) stems from the power dissipated in a LC cell due to dielectric losses, it is believed that this equation is still valid and can be in use to characterize the increase in temperature in our designated cell by dielectric heating from the pseudo-dielectric relaxation displayed in Fig. 2(a).

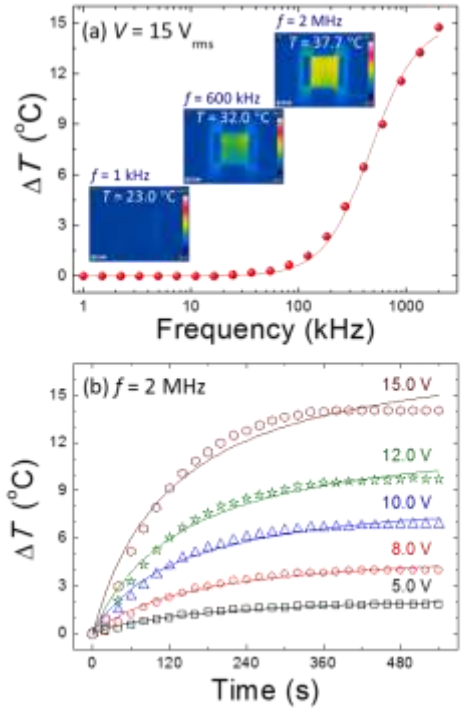

FIG. 3. (a) Temperature increase as a function of the frequency of an applied AC voltage of 15 V_{rms} and (b) dynamic temperature increases of the CLC cell under the application of various voltages at a fixed frequency of 2 MHz. Note that the solid line in (a) is a simulated curve based on Eq. (6) and that the open symbols and solid lines in (b) represent experimental and curve-fitting results according to Eq. (5), respectively.

By setting t $\rightarrow\infty$, Eq. (5) in the stationary state can be simplified as [22]:

$$\Delta T = \left(\frac{V^2 A\varepsilon_0(\varepsilon_s - \varepsilon_\infty)}{dh}\right)\left(\frac{\tau_R \omega^2}{1+\omega^2\tau_R^2}\right). \quad (6)$$

While fitting the experimental data (represented by spherical symbols) from Fig. 3(a) with Eq. (6), one can find that the fitting curve of $\Delta T(t)$ (solid line in Fig. 3(a)), with the parameters h ~0.055 W·K^{-1} and τ_R ~3.4 × 10^{-7} s, is in line with the measured data (yielding the corresponding coefficient of determination R^2 = 0.99). Notably, the f_R value of ~467 kHz calculated from τ_R is very close to f_{PR} = 467 kHz at T = 35.3 °C or f_{PR} = 472.5 kHz at T = 37.7 °C (see Fig. 2(b)). Moreover, Fig. 3(b) delineates time-evolved temperature changes of the cell driven by various voltages at f = 2 MHz. Again, these observations were performed at T_s = 23 °C. For a given voltage, the temperature increased monotonically with increasing dielectric heating time, reaching a saturated value and becoming saturated at t > 360 s. These results can be properly fitted to Eq. (5) with $R^2 \geq 0.97$. For each fitting curve in Fig. 3(b), C and h are adjustable parameters. Because the relation of $f_R = f_{PR}$ is verified based on fitting results of Fig. 3(a), τ_R here is considered as a fixed value and is given from $\tau_R = (2\pi f_{PR})^{-1}$ at its saturated temperature, extracted from Fig. 2(b) (e. g., f_{PR} = 470.8 kHz at T = 37.0 °C for V = 15 V_{rms} or f_{PR} = 461.3 kHz at T = 32.7 °C for V = 12 V_{rms}). The fitting results indicate that C is nearly constant at various voltage conditions, yielding C = 5.6 ± 0.4 J·K^{-1}. This is understandable because C is primarily dictated by the thermal properties of the ITO-substrates and the LC layer which are virtually unaffected by the external voltage. The findings unraveled in Fig. 3 suggest that the heat generation in the designated CLC cell is ascribed to the generation of dielectric losses from the equivalent R_{ITO}–C_{cell} circuit through the dielectric heating effect. Although a rigorous mechanism behind the dielectric heating behavior from the cell-geometry-dominated dielectric relaxation is still underway in this laboratory, the experimental results reported in the present work can theoretically be formulated by Eq. (5), giving a general approximation describing the temperature increase arising from the dielectric heating.

The pseudo-dielectric relaxation from the ITO effect has long been considered as a nuisance for dielectric investigations of a LC in that signals of certain relaxations from the LC material could be concealed at high frequencies [23]. Because the pseudo-dielectric relaxation can hardly be avoided in a sandwich-type cell, the direct way to suppress or shift this undesired dielectric signal beyond the investigated frequency regime is to use metal substances instead of ITO to lower the resistivity of the electrodes (e.g. silver electrode used in Ref. 16) and/or to increase the cell gap (e.g. d = 40 μm used in Ref. 17), according to Eq. (1). Some other methods based on mathematical calculations have also been proposed to eliminate the contribution of the cell-geometry-induced pseudo signal to the complex dielectric spectra so as to deduce the real dielectric behaviors of LCs [19, 23]. Since the dielectric heating behavior in a LC cell has only been focused on the dielectric relaxation from dual-frequency LC molecules, the present work would be the first of its kind confirming the contribution of the LC container to dielectric heating.

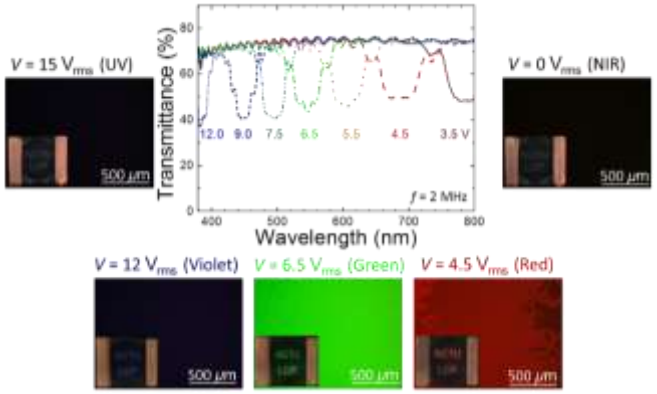

FIG. 4. Transmission spectra, texture images of the CLC and photographs of the real cell driven by various voltages at 2 MHz.

Utilizing this unique feature together with the thermal-responsive bandgap properties of a CLC, one can electrically tune the reflection band of the negative CLC through the control of cell temperature by an externally applied voltage. Figure 4 displays transmission spectra and optical textures together with the corresponding photographs of the cell submitted to various AC voltages at f = 2 MHz. Taken without any polarizer, these photographs shown as the insets are mirror images of a piece of black paper showing white inverted letters ("NCTU LCP") reflected from the CLC cell. To illustrate the wavelength tuning ability, we referred to Fig. 1(a) and masterly controlled T_s = 22 °C so as to allow the reflection band to lie in the near IR region in the field-off state (λ_c = 1392 nm at V = 0 V_{rms}). When the voltage increased to 3.5 V_{rms}, the bandgap appeared in the visible light regime (λ_c ~ 800 nm at V = 3.5 V_{rms}) and blue-shifted further with increasing voltage, reaching λ_c ~ 380 nm at V = 12 V_{rms}. The color change of the reflective optical texture and of the cell appearance from red at V = 4.5 V_{rms} to green at V = 6.5 V_{rms}, blue at V = 9 V_{rms} and to violet at V = 12 V_{rms} are consistent with the corresponding bandgap properties. Further increasing the voltage to 15 V_{rms} resulted in the disappearance of the bandgap from the visible spectrum.

The bandgap shift to the UV region at V = 15 V_{rms} brought about the dark appearance of the CLC phase. The results as shown in Fig. 4 imply that the proposed electrical tuning method enables a broadband tunable wavelength range, spanning from the IR, visible, and UV light regions, for reflective color by simply regulating the applied voltage between 0 and 15 V_{rms} at f = 2 MHz.

Alternatively, Fig. 5(a) depicts the frequency dependence of tunable λ_c of the cell under the application of various external voltages. In considering the limit of detection of the used spectrometer (i.e., 380 nm–820 nm), T_s here was set at ~23 °C so that λ_c ~760 nm at V = 0 V_{rms}. It is clear that λ_c remained unchanged and then decreased with ascending frequency beyond a critical value (f_0), dropping with increasing V from f_0 ~118 kHz at V = 5 V_{rms} and approaching a saturated value of f_0 ~24.5 kHz at voltages beyond 12 V_{rms}. This establishes that both the amplitude (Fig. 4) and frequency (Fig. 5(a)) of the voltage have a profound influence on λ_c of the reflection band. The higher the amplitude (frequency) of the voltage applied across the cell gap, the lower the frequency (amplitude) required for desired λ_c

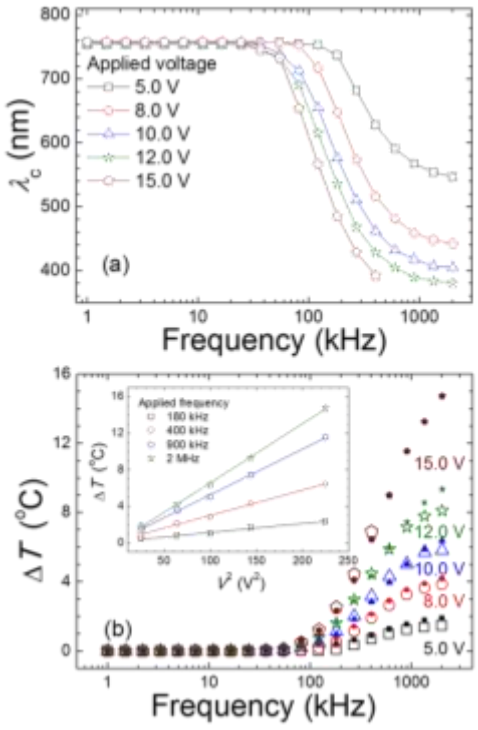

FIG. 5. Frequency-dependent (a) center wavelength and (b) temperature elevation at various AC voltages. The open and solid symbols in (b) represent ΔT deduced from fitting of the experimental data using Eq. (2) and measured with an IR camera, respectively.

tuning (see Eq. (6)). For instance, to achieve tunable λ_c from 760 nm to 380 nm, one can vary the frequency from 24.5 kHz to 2 MHz at V = 12 V_{rms} or from 24.5 kHz to 403.7 kHz at V = 15 V_{rms}. Furthermore, Fig. 5(b) presents the frequency dependence of ΔT of the cell applied with various voltages. The ΔT data, obtained by fitting the results of Fig. 5(a) into Eq. (2), nicely match the (solid-symbol) curves acquired by IR thermography, corroborating the change in λ_c by voltage-induced temperature alteration. Notice that the $\Delta T(f)$ curves at various voltages can be plotted by fitting the data using Eq. (6) as well (not shown in the figure). In addition, one can see from the inset of Fig. 5(b) that ΔT is linearly proportional to the square of V, conforming to the mechanism of the dielectric heating effect as described by Eq. (6). Furthermore, to verify that the abovementioned results are non-specific, we prepared another CLC cell, designated CLC-1, whose ITO resistivity (giving R_{ITO} ~1.6 kΩ) is much larger than that of the primarily used cell (R_{ITO} ~310 Ω) in this study, whereas other conditions, such as A = 1 cm^2, d = 5 μm and the CLC injected, for these two cells are kept identical. Figure 6 shows the dielectric spectra of CLC-1 at T = 23 °C (Fig. 6(a)) and the frequency-dependent λ_c and ΔT of this cell under the application of a 15-V_{rms} voltage (Fig. 6(b)). One can still observe from Fig. 6(a) a single Debye-like dielectric relaxation but it shifts to lower frequencies as compared with that of results shown in Fig. 2(a). By fitting the real-part dielectric spectrum into Eq. (3), the results indicate an identical value of ε_s = 6.4 and a decrease in f_{PR} (from 440 kHz to 93 kHz) upon increasing the value of R_{ITO} (from 310 Ω to 1.8 kΩ). This confirms again that the unique dielectric relaxation in the complex dielectric spectra of our used CLC

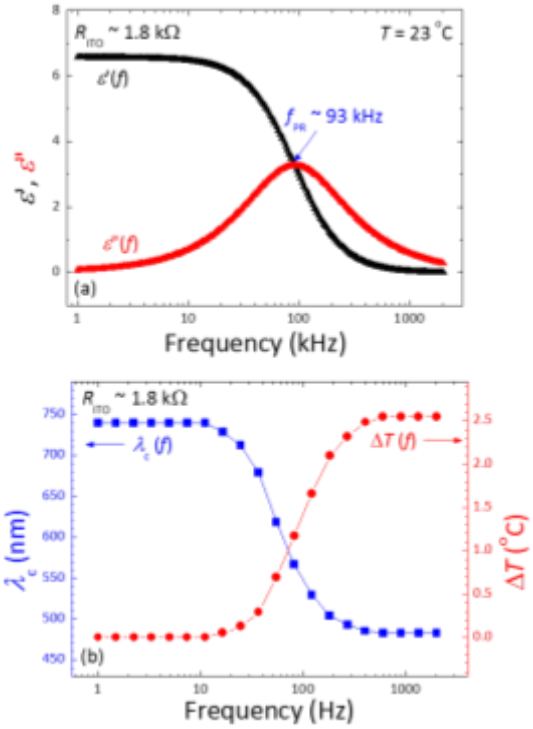

FIG. 6. (a) Complex dielectric spectra of the CLC cell with R_{ITO} = 1.6 kHz at T = 23 °C and (b) frequency-dependent λ_c and ΔT of this cell under a 15-V applied voltage.

cell is attributable to the significant R_{ITO}–C_{cell} circuit of the cell rather than the rotation of LC molecules. Moreover, electrically tunable λ_c of CLC-1 can also be realized but its tunable range (between 740 nm and 480 nm) by 15-V_{rms} voltage in the frequency range between 1 kHz and 2 MHz is narrower than that of the CLC with R_{ITO} ~310 Ω (between 760 nm to 380 nm) even by V = 12 V_{rms} in the same frequency range, as shown in Fig. 6(b). Similarly, we obtain ΔT by the variation in λ_c according to Eq. (2). As displayed in Fig. 6(b), the frequency-dependent ΔT curve of CLC-1 can perfectly be fitted by Eq. (6) with f_R = 91.2 kHz which still follows the relation of f_R ~ f_{PR} = 93 kHz. The frequency-dependent ΔT also reflects a weakened efficacy of dielectric heating of CLC-1 by lowered f_R; this is again in consistence with Eq. (6). Additionally, experiments using cells with various cell parameters have also been performed in our laboratory. It can be summarized based on the data that the cell gap, the electrode area, and the intrinsic dielectric anisotropy of LC materials can be used to optimize the pseudo-dielectric relaxation and the strength of dielectric heating, following Eqs. (1) and (5), respectively.

4. CONCLUSIONS

In summary, we have demonstrated a feasible approach enabling the electrically tunable reflective color from a CLC over the full visible spectrum. According to the thermally sensitive bandgap properties of the CLC and the cell parameters, the working principle of this approach is explicated in terms of the tunable λ_c of the Bragg reflection band via the voltage-induced dielectric heating effect instead of the Joule heat. Notably, the dielectric heating is predominated by the pseudo-dielectric relaxation originating from the use of the ITO cell with finite conductance. This heating effect is unique and demonstrated for its first time in this study, which should be carefully distinguished from the well-known dielectric heating effect in dual-frequency LCs explained by the dipole rotation of the molecules. Upon the application of AC voltage to the cell, our results validate that the tunable color (380 nm ≤ λ_c ≤ 780 nm) can be readily realized by varying either the voltage amplitude (say, 0 V_{rms} ≤ V ≤ 12 V_{rms} at f = 2 MHz) or frequency (e.g., 24.5 kHz ≤ f ≤ 2 MHz at V = 12 V_{rms}). Because the CLC exhibits electro-thermally tunable λ_c between 340 nm at 0 V_{rms} and 1392 nm at 15 V_{rms} with a frequency of 2 MHz, true black color can be facilely obtained. The fabrication of the proposed negative CLC cell is of ease by virtue of all materials used, including the empty sandwich-type cells with ITO substrates, to be commercially available. In contrast to other electrical tuning methods, this study provides a new pathway to a wider tunable reflective color range with lower operating voltage, promoting the applicability of CLC for the design of superior color-reflective displays and electrically tunable photonic devices.

ACKNOWLEDGMENTS

This study was financially supported by the Ministry of Science and Technology, Taiwan, through Grant Nos. 104-2112-M-009-008-MY3 and 106-2923-M-009-002-MY3.

REFERENCES

1. D.-K. Yang, J. L. West, L.-C. Chien, and J. W. Doane, "Control of reflectivity and bistability in displays using cholesteric liquid crystals," J. Appl. Phys. **76**, 1331–1333 (1994).
2. N. Y. Ha, Y. Ohtsuka, S. M. Jeong, S. Nishimura, G. Suzaki, Y. Takanishi, K. Ishikawa, and H. Takezoe, "Fabrication of a simultaneous red–green–blue reflector using single-pitched cholesteric liquid crystals," Nat. Mater. **7**, 43–47 (2008).
3. Y. Matsuhisa, Y. Huang, Y. Zhou, S.-T. Wu, R. Ozaki, Y. Takao, A. Fujii, and M. Ozaki, "Low-threshold and high efficiency lasing upon band-edge excitation in a cholesteric liquid crystal," Appl. Phys. Lett. **90**, 091114 (2007).
4. C.-K. Chang, S.-W. Chiu, H.-L. Kuo, and K.-T. Tang, "Cholesteric liquid crystal-carbon nanotube hybrid architectures for gas detection," Appl. Phys. Lett. **100**, 043501 (2012).
5. G. Chilaya, *Cholesteric Liquid Crystals: Optics, Electro-optics, and Photo-optics*, in *Chirality in Liquid Crystals*, edited by H.-S. Kitzerow and C. Bahr (Springer, New York, 2001), Ch. 6, pp. 159–185.
6. F. Zhang and D.-K. Yang, "Temperature dependence of pitch and twist elastic constant in a cholesteric to smectic A phase transition," Liq. Cryst. **29**, 1497–1501 (2002).
7. Z. Cheng, K. Li, R. Guo, F. Wang, X. Wu, L. Zhang, J. Xiao, H. Cao, Z. Yang, and H. Yang, "Bandwidth-controllable reflective polarisers based on the temperature-dependent chiral conflict in binary chiral mixtures," Liq. Cryst. **38**, 233–239 (2011).

8. Y. Huang, Y. Zhou, C. Doyle, and S.-T. Wu, "Tuning the photonic band gap in cholesteric liquid crystals by temperature-dependent dopant solubility," Opt. Express **3**, 1236–1242 (2006).
9. T. J. White, M. E. McConney, and T. J. Bunning, "Dynamic color in stimuli-responsive cholesteric liquid crystals," J. Mater. Chem. **20**, 9832–9847 (2010).
10. T.-H. Lin, C.-H. Chen, Y. Chen, T. Wei, C.-W. Chen, and A. Y.-G. Fuh, "Electrically controllable laser based on cholesteric liquid crystal with negative dielectric anisotropy," Appl. Phys. Lett. **88**, 061122 (2006).
11. C. A. Bailey, V. P. Tondiglia, L. V. Natarajan, M. M. Duning, R. L. Bricker, R. L. Sutherland, T. J. White, M. F. Durstock, and T. J. Bunning, "Electromechanical tuning of cholesteric liquid crystals," J. Appl. Phys. **107**, 013105 (2010).
12. L. V. Natarajan, J. M. Wofford, V. P. Tondiglia, R. L. Sutherland, H. Koerner, R. A. Vaia, and T. J. Bunning, "Electro-thermal tuning in a negative dielectric cholesteric liquid crystal material," J. Appl. Phys. **103**, 093107 (2008).
13. S. S. Choi, S. M. Morris, W. T. S. Huck, and H. J. Coles, Wavelength tuning the photonic band gap in chiral nematic liquid crystals using electrically commanded surfaces,"" Appl. Phys. Lett. **91**, 231110 (2007).
14. S. S. Choi, S. M. Morris, W. T. S. Huck, and H. J. Coles, "Electrically tuneable liquid crystal photonic bandgaps,"Adv. Mater. **21**, 3915–3918 (2009).
15. J. Xiang, Y. Li, Q. Li, D. A. Paterson, J. M. D. Store, C. T. Imrie, and O. D. Lavrentovich, "Electrically tunable selective reflection of light from ultraviolet to visible and infrared by heliconical cholesterics," Adv. Mater. **27**, 3014–3018 (2015).
16. M. Schadt, "Dielectric heating and relaxations in nematic liquid crystals," Mol. Cryst. Liq. Cryst. **66**, 319–336 (1981).
17. C.-H. Wen and S.-T. Wu, "Dielectric heating effects of dual-frequency liquid crystals," Appl. Phys. Lett. **86**, 231104 (2005).
18. Y. Yin, S. V. Shiyanovskii, and O. D. Lavrentovich, "Electric heating effects in nematic liquid crystals," J Appl. Phys. **100**, 024906 (2006).
19. P. Perkowski, D. Lada, K. Ogrodnik, J. Rutkowska, W. Piecek, and Z. Raszewski, "Technical aspects of dielectric spectroscopy measurements of liquid crystals," Opto-Electron. Rev. **16**, 271–276 (2008).
20. S.-Y. T. Tzeng, C.-N. Chen, and Y. Tzeng, "Thermal tuning band gap in cholesteric liquid crystals," Liq. Cryst. **37**, 1221–1224 (2010).
21. P. N. Keating, "A theory of the cholesteric mesophase" Mol. Cryst. Liq. Cryst. **8**, 315–326 (1969).
22. Y.-C. Hsiao, Z.-H. Yang, D. Shen, and W. Lee, "Technical aspects of dielectric spectroscopy measurements of liquid crystals," Adv. Opt. Mater. **6**, 1701128 (2018).
23. P. Perkowski, "How to determine parameters of soft mode from dielectric spectroscopy performed using cells with ITO electrodes?" Opto-Electron. Rev. **19**, 76–82 (2011).